

# Casting Solvent Effect on Crystallization Behavior and Morphology of Poly(ethylene oxide)/Poly(methyl methacrylate)

W. B. LIAU, C. F. CHANG

Institute of Materials Science and Engineering, National Taiwan University, Taipei, Taiwan, Republic of China

Received 5 August 1999; accepted 22 October 1999

**ABSTRACT:** Poly(ethylene oxide) (PEO)/poly(methyl methacrylate) (PMMA) blends were prepared by casting from either chloroform or benzene solvents. After casting from solvents, all samples used in this study were preheated to 100°C and held for 10 min. Then, the solvent effect on the crystallization behavior and thermodynamic properties were studied by differential scanning calorimeter (DSC). Also, the morphology of spherulite of casting film was studied by polarized optical microscope. From the DSC and polarizing optical microscopy (POM) results, it was found that PEO/PMMA was miscible in the molten state no matter which casting solvent was used. However, the crystallization of PEO in the chloroform-cast blend was more easily suppressed than it was in the benzene-cast blend. Relatively, the chloroform-cast blend showed the greater melting-point depressing of PEO crystals. Also, the spherulite of chloroform-cast film showed a coarser birefringence. It was supposed that the chloroform-cast blend had more homogeneous morphology. It is fair to say that polymer blends, cast from solvent, are not necessarily in equilibrium. However, the benzene-cast blends still were not in equilibrium even after preheating at 100°C for 10 min. © 2000 John Wiley & Sons, Inc. *J Appl Polym Sci* 76: 1627–1636, 2000

**Key words:** solvent effect in the miscibility; poly(ethylene oxide); poly(methyl methacrylate); polymer blend

## INTRODUCTION

Blending polymers is an efficient and economic method to develop new polymeric materials.<sup>1–2</sup> Many miscible polymer blends have been found. One such polymer blend, poly(ethylene oxide)/poly(methyl methacrylate) (PEO/PMMA), containing the interaction between ether and ester groups, proved to be miscible from the observation of their single-composition-dependent glass transition temperatures and melting-point de-

pressing of PEO. Their crystallization kinetics, thermodynamic properties, and morphology have been extensively studied by means of differential scanning calorimeter (DSC), optical microscopy (POM), small-angle X-ray scattering (SAXS), and small-angle neutron scattering (SANS).<sup>3–6</sup> Also, effects of the molecular weight<sup>4,7</sup> and tacticity<sup>8–11</sup> of PMMA on the blends were studied.

Because the miscibility of polymer blends is one of the major effects on properties of blends, the subject of miscibility of polymer blends has gained much attention.<sup>1,2</sup> The blend miscibility is quite dependent on the method of preparation. Most of blends reported in the literature were cast from solution. In the cases of PEO/PMMA blends, chloroform was the most frequently used casting solvent. Although it was expected that the casting

---

Correspondence to: W. B. Liao.

Contract grant sponsor: National Science Council; contract grant number: NSC86-2216-E-002-007.

*Journal of Applied Polymer Science*, Vol. 76, 1627–1636 (2000)  
© 2000 John Wiley & Sons, Inc.

**Table I Materials and Their Characteristics**

Code	Description	Source
PEO	Poly(ethylene oxide), $M_w = 200,000$	Aldrich Chemical Company
PMMA	Poly(methyl methacrylate), $M_w = 120,000$	Aldrich Chemical Company

solvent would influence the blend miscibility and thus the properties of blends, limited articles studying the solvent effect on the properties of blends were published.<sup>12–19</sup> The solvent effect on the miscibility of polystyrene/poly(vinyl methyl ether) blends was investigated.<sup>14</sup> The results showed that the blend cast from toluene or benzene was compatible, whereas incompatible blend was obtained on casting from chloroform. For the PMMA/poly(vinyl acetate) (PVAc) blend, it was reported<sup>17–19</sup> as a miscible blend when chloroform was used as a casting solvent and as an immiscible blend when *N,N*-dimethyl formamide or tetrahydrofuran were used. However, the miscibility of PMMA/PVAc blend depends on the casting temperature when the solvent, toluene, was used.<sup>19</sup> For the PEO/PVAc blends, the compatible blends were obtained on casting from benzene or chloroform according to the observation of their single composition-dependent glass transition temperatures of blends. However, the benzene-cast blends had more homogeneous morphology, and the crystallization of PEO was more easily suppressed than it was in the chloroform-cast blends.<sup>12</sup> Radhakrishnan and Venkatachalapathy reported that the crystallinity and the intensities of the peaks of wide-angle X-ray diffraction (WAXD) of PEO/PMMA were influenced by different casting solvent.<sup>13</sup> The authors suggested that a different solvent providing the different constrained morphology gives rise to the changes in the WAXD. However, they did not study the solvent effect on the radius growth rate and morphology of PEO spherulites. In this study, the crystallization and morphology of PEO in the PEO/PMMA blends cast from benzene or chloroform were studied by means of DSC and POM.

## EXPERIMENTAL

### Materials and Blend Preparation

The materials used in this work and their characteristics were given in Table I. The PEO was predried in a vacuum oven at 50°C for 1 day

before use. Also, the PMMA was pretreated in a vacuum oven at 140°C for 1 day before use. Then, certain amounts of PEO and PMMA were dissolved in benzene or chloroform according to the desired composition. The total polymer concentration was 1 g/100 mL solvent. The solution was continuously stirred for 2 days at room temperature and then poured onto the glass plate. The solvent was evaporated very slowly under ambient condition at room temperature. Finally, a blend film of ~ 0.08 mm in thickness was obtained. The sample film or chip was dried in a vacuum oven at 45°C for at least 1 week to remove the residual solvent (more time required for benzene-cast blends). TGA was used to check the residual solvent in the final blend film. The results showed no measurable residual solvent in the samples. All samples cast from solvent were preheated to 100°C and held at that temperature for 10 min before the following experiments were carried out.

### Glass Transition Temperature Measurement

Glass transition temperature ( $T_g$ ) measurements were carried out by using a Du Pont (Wilmington, DE) differential scanning calorimeter (Model 910). Indium and *n*-heptane were used as standards for temperature calibration. Samples of ~ 8 mg loaded in aluminum cells were heated to 100°C for 10 min to melt PEO crystals, followed by quenching to ~ 130°C, and then scanned to 150°C with a heating rate of 10°C/min.  $T_g$  was determined from the half-height point of the step change in the thermogram and the error was within 2°C.

### Isothermal Crystallization and $t_{1/2}$ Measurement

The isothermal crystallization experiments were carried out by using a Perkin–Elmer differential scanning calorimeter (Model DSC-7). Indium and *n*-heptane were used as standards for temperature calibration. About 8 mg of sample was heated to 100°C to melt crystals, and the temperature was held for 10 min to completely melt the crys-

tals. The sample was cooled to a desired crystallization temperature at a cooling rate of 80°C/min. After completely crystallizing, the time required to accomplish 50% crystallization was recorded as  $t_{1/2}$ .

### Melting-Point Measurement and Morphology Observation

Samples used for POM were pressed by glass cover slip above the melting point in hot-stage. The resultant films were approximately 10  $\mu\text{m}$  in thickness. The optical micrographs were obtained by using a Zeiss polarizing microscope equipped with a Linkam THMS 600 hot-stage. All samples were preheated at 100°C for 10 min to melt the PEO crystals. Then the samples were quenched to the desired crystallization temperature at a cooling rate of 130°C/min. Spherulitic growth was monitored by using a video camera mounted on the microscope and analyzed by a digital image analyzer. The video frames were captured and stored by image analysis software to determine the variation of spherulitic diameters with time in different crystallization temperatures. Thereby, growth rates were obtained from the linear regression of the spherulite radius as a function of time. At the same time, the morphology of PEO spherulites was observed. After the completion of spherulite growth, the samples were heated again at 2°C/min to measure the melting point of PEO crystals. The melting point was the temperature at which the last spherulite disappeared (disappearance of birefringence).

## RESULTS AND DISCUSSION

One thing that must be mentioned is that all samples were preheated to 100°C and held at that temperature for 10 min before the DSC and POM experiments.

DSC thermograms of the PEO/PMMA blends cast from benzene are shown in Figure 1. There was a sharp thermal transition at  $\sim 110^\circ\text{C}$  for the neat PMMA. It was the  $T_g$  of PMMA. The  $T_g$  of neat PEO was ambiguous because of the high crystallinity. However, a sharp melting peak was shown in DSC thermograms for the neat PEO, and the melting temperature was  $\sim 67^\circ\text{C}$ . Up to 30% PEO contents, the blends showed no crystallization during the quenching and heating processes. Thus, they were totally amorphous. For the PEO/PVAc system, the PEO crystal formed even when the PEO content was 20%.<sup>12</sup> Obvi-

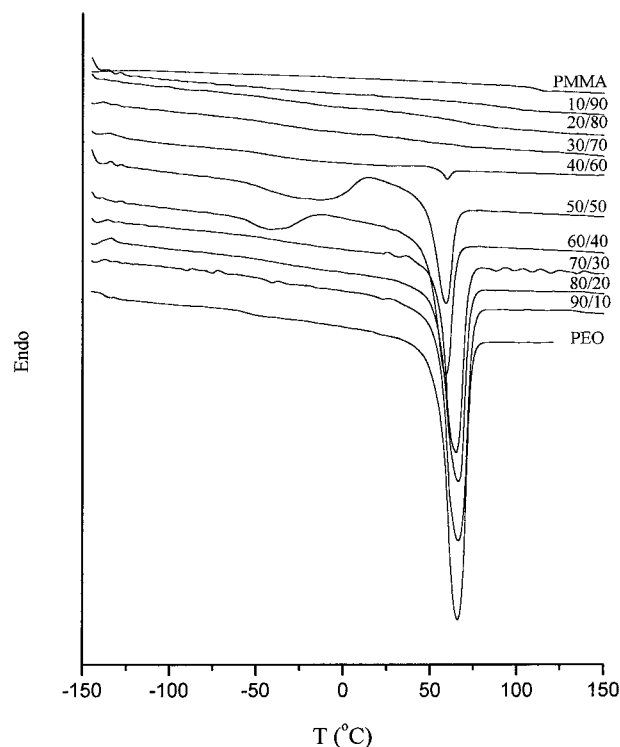


**Figure 1** DSC thermograms of PEO/PMMA blends cast from benzene.

ously, the PMMA had a better ability to suppress the crystallization of PEO in blends than PVAc. The glass transition of PMMA was higher than the glass transition of PVAc.

For the blends with 40–60% PEO, the thermograms showed exothermic peaks following the glass transition. This indicated that recrystallization occurred in these blends during the heating process. The total recrystallization heat ( $\Delta H_{rc}$ ) and fusion heat ( $\Delta H_f$ ) of the PEO in these blends were obtained by integrating the areas under the recrystallization and melting peaks of DSC curves, respectively. The results are listed in Table II. From the ratio of  $\Delta H_f$  and  $\Delta H_{rc}$ , it was shown that the PMMA could hardly suppress the crystallization of PEO in these blends during the quenching process. For the above blends, a single  $T_g$  decreased with increasing the PEO content. This indicated that the blends were miscible in the molten state. It was difficult to quantitatively discuss the breadth of the glass transition, because the recrystallization occurred immediately after the glass transition. However, the glass transitions of the blends were much broader than that of neat PMMA. It indicated that a wide distribution of molecular-motion environments ex-

**Table II Thermal Behaviors of Blends**

PEO/PMMA (wt %)	Chloroform-Cast			Benzene-Cast		
	$T_g$ (°C)	$T_m$ (°C)	$\Delta H_{rc}/\Delta H_f$	$T_g$ (°C)	$T_m$ (°C)	$\Delta H_{rc}/\Delta H_f$
100/0	— <sup>a</sup>	67	—	—	67	—
90/10	—	66	—	—	66	—
80/20	—	65	—	—	66	—
70/30	—	64	—	—	65	—
60/40	-52	60	0.60	-52	59	0.49
50/50	-46	58	0.84	-44	59	0.79
40/60	-38	59	0.92	-38	59	0.82
30/70	-30	—	—	-34	—	—
20/80	66	—	—	69	—	—
10/90	92	—	—	95	—	—
0/100	110	—	—	110	—	—

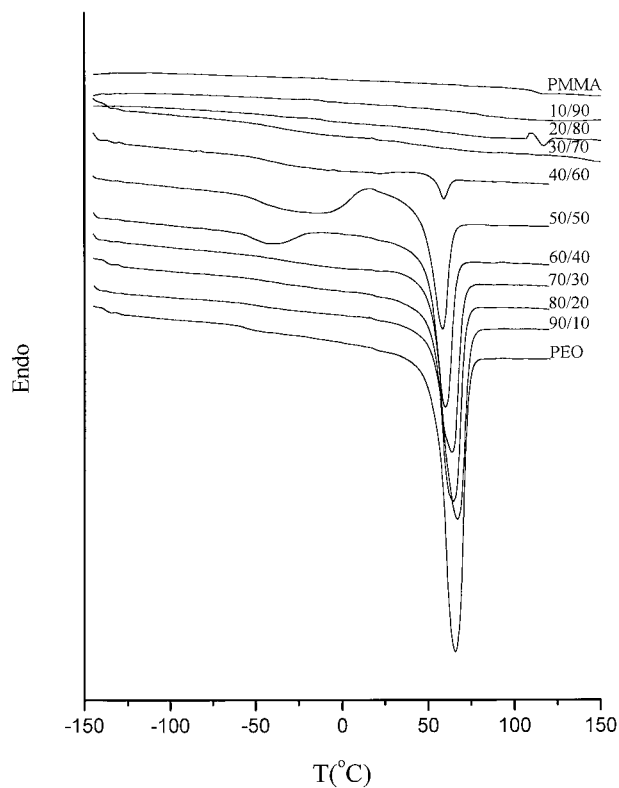
<sup>a</sup> —, very small or not obtained.

isted in blends, although the blends were macroscopically homogeneous.

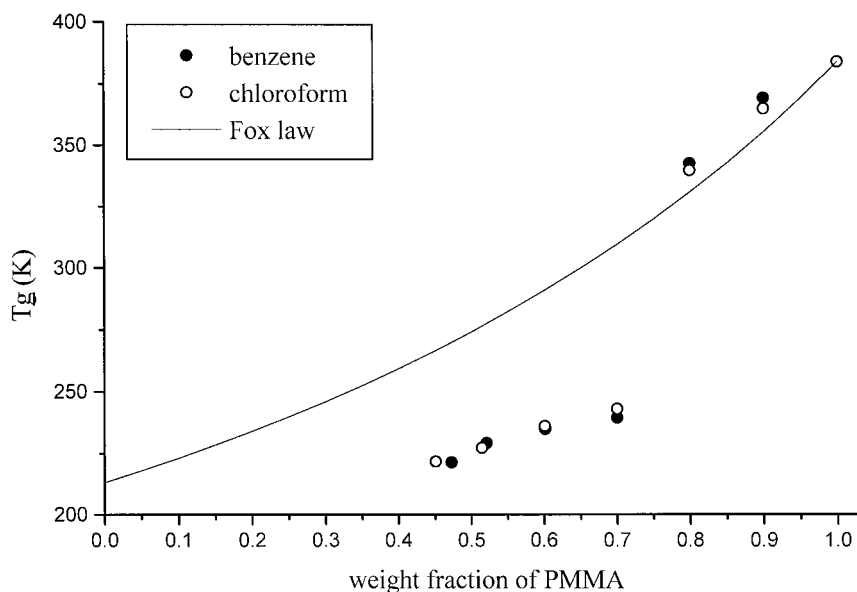
For the blends with 70–90% PEO, the thermograms showed no recrystallization (i.e., all of the crystals were formed during the quenching process). For these blends, the  $T_g$  was ambiguous because of the high crystallinity as neat PEO.

Figure 2 shows the DSC results of PEO/PMMA blends cast from chloroform. A comparison of Figures 1 and 2 shows that the thermograms of chloroform-cast blends are similar to those of benzene-cast blends. From Table II, it is also shown that the  $T_g$ 's and melting points of blends prepared from different solvents were about equal. The single-composition-dependent  $T_g$  was observed in chloroform-cast blends. Again, it indicated that chloroform-cast blends were miscible in the molten state. Thus, benzene-cast and chloroform-cast blends were homogeneous based on the scale of glass transition motion. However, for 60/40, 50/50, and 40/60 blends, it is shown from Table II that the ratios of recrystallization and fusion heats of chloroform-cast blends were different from those of benzene-cast blends. The values of  $\Delta H_{rc}/\Delta H_f$  for chloroform-cast blends were greater than those observed in benzene-cast blends. Thus, the crystallization of PEO during the quenching process was suppressed more easily in the chloroform-cast blends. It was supposed that the chloroform-cast blends had more homogeneous morphology on the microscopic scale. Furthermore, the differences in the values of  $\Delta H_{rc}/\Delta H_f$  for PEO/PMMA blends were not as large as they were for the PEO/PVAc blends.<sup>12</sup>

Figure 3 shows the relation between the  $T_g$  and amorphous composition of PEO/PMMA blends. Because it was difficult to obtain the completely amorphous blends by the quenching process for some blends, the single  $T_g$  measured by DSC cor-



**Figure 2** DSC thermograms of PEO/PMMA blends cast from chloroform.



**Figure 3** Glass transition temperature versus weight fraction of PMMA plot for the PEO/PMMA blends.

responded to the amorphous phase composition, not the composition of blends. Thus, the composition of the amorphous phase was calculated by using the relation:

$$w_a = \frac{w_b - [(\Delta H_f - \Delta H_{rc})/\Delta H_f^0]}{1 - [(\Delta H_f - \Delta H_{rc})/\Delta H_f^0]} \quad (1)$$

The  $w_a$  and  $w_b$  were PEO weight fractions in amorphous phase and blend, respectively.  $\Delta H_{rc}$  and  $\Delta H_f$  were the apparent enthalpy of recrystallization and melting per gram of PEO in the blend.  $\Delta H_f^0$  was the heat of melting per gram of perfect PEO crystal (from literature data,  $\Delta H_f^0 = 196.46 \text{ J/g}^{20}$ ), respectively. It became obscure when the PMMA content was  $<40\%$ . Thus, their  $T_g$  values were not shown in Figure 3. The experimental value of  $T_g$  of neat PEO was reported to be in the range  $-45$  to  $-60^\circ\text{C}$  in the literature.<sup>3,6,7,21–28</sup> The solid line in Figure 3 represented the  $T_g$  values of the blends estimated from the Fox equation,

$$\frac{1}{T_g} = \frac{w_1}{T_{g1}} + \frac{w_2}{T_{g2}} \quad (2)$$

where  $T_g$ ,  $T_{g1}$ , and  $T_{g2}$  were the glass transition temperatures of the blend, neat component 1 and 2, respectively;  $w_1$  and  $w_2$  were the weight fractions of component 1 and 2 in the blend. The  $T_g$  of

PMMA was  $110^\circ\text{C}$ . The  $T_g$  of PEO was assumed to be  $-60^\circ\text{C}$ .<sup>7</sup> It is important to note that above 30% PEO, the  $T_g$  was only weakly dependent on composition and was quite close to that of the neat PEO. Such unusual behavior of glass transition was reported in the literature.<sup>4,28,29</sup> Alfonso and Russell proposed that the reason for this unusual behavior was that the  $T_g$  observed was not the true  $T_g$  of the blend but rather a relaxation associated with the crystal/amorphous interface.<sup>4</sup> The true  $T_g$  would be close to the melting point of PEO crystal. Thus, the true  $T_g$  was difficult to be observed. However, there was no doubt that the PEO/PMMA blend was miscible from the NMR relaxation time measurements in the melt.<sup>30</sup> From the NMR experiment, a single  $T_1$  relaxation

**Table III**  $T_{1/2}$  (min) at Various  $T_c$  for PEO/PMMA Blends

PEO/PMMA (wt %)	Chloroform-Cast		Benzene-Cast	
	40°C	44°C	40°C	44°C
90/10	5.8	16.5	3.0	9.6
80/20	11.2	36.7	7.1	22.3
70/30	38.3	80.7	19.8	46.9
60/40	174.6	— <sup>a</sup>	55.8	91.3

<sup>a</sup> —, value not obtained.

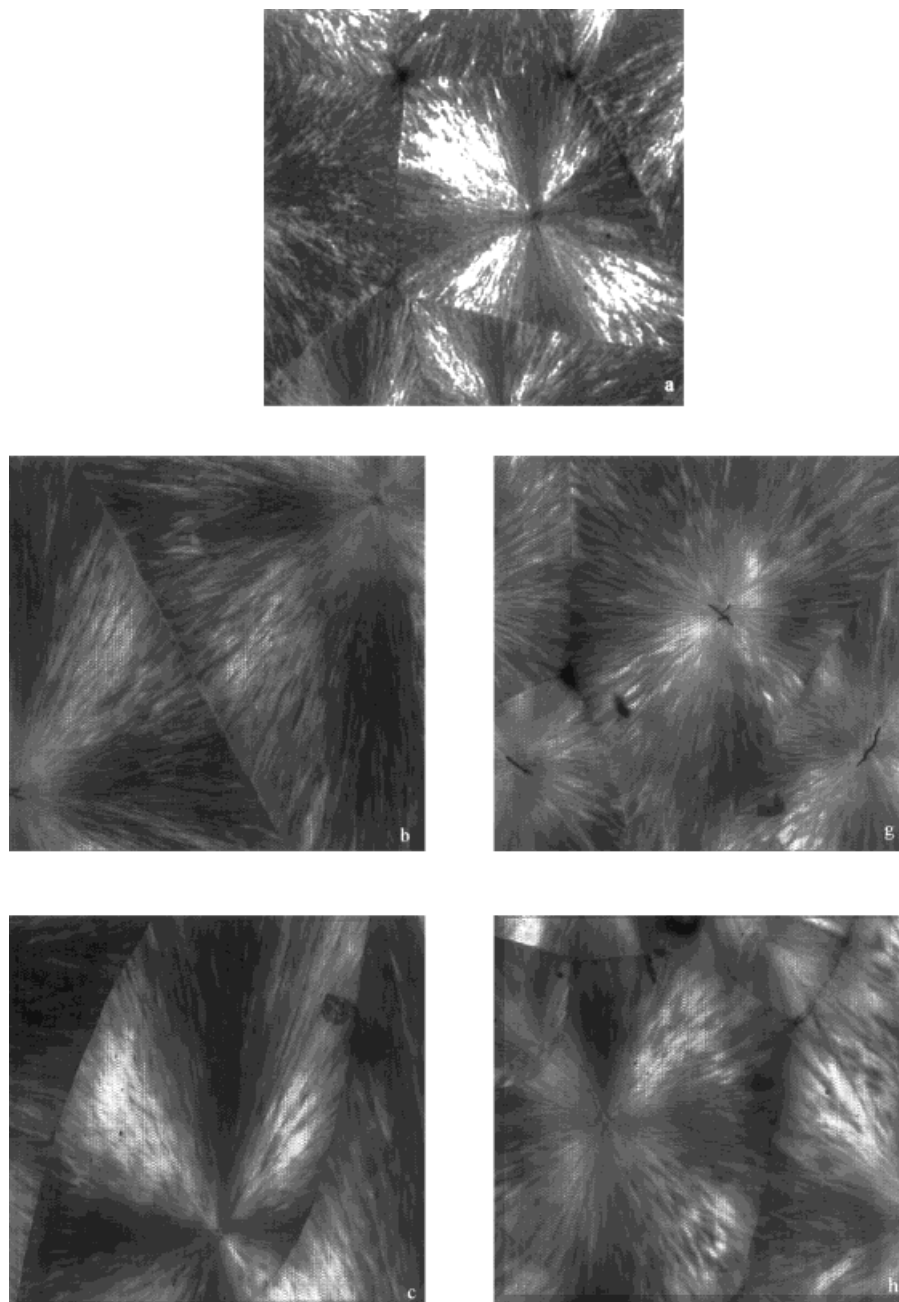


**Figure 4** Optical micrographs of spherulites in PEO and PEO/PMMA blends of various composition: (a) PEO; (b) chloroform-cast PEO/PMMA (90/10); (c) chloroform-cast PEO/PMMA (80/20); (d) chloroform-cast PEO/PMMA (70/30); (e) chloroform-cast PEO/PMMA (60/40); (f) chloroform-cast PEO/PMMA (50/50); (g) benzene-cast PEO/PMMA (90/10); (h) benzene-cast PEO/PMMA (80/20); (i) benzene-cast PEO/PMMA (70/30); (j) benzene-cast PEO/PMMA (60/40); (k) benzene-cast PEO/PMMA (50/50).

time was found, suggesting miscibility in the melt.

The isothermal crystallization behaviors of benzene- and chloroform-cast blends were studied by DSC. The time required to finish 50% crystal-

lization was called half-time of crystallization and denoted as  $t_{1/2}$ . Table III shows the values of  $t_{1/2}$  of the neat PEO and its blends. The values of  $t_{1/2}$  increased with increasing PMMA content and increasing the crystallization temperature. It was

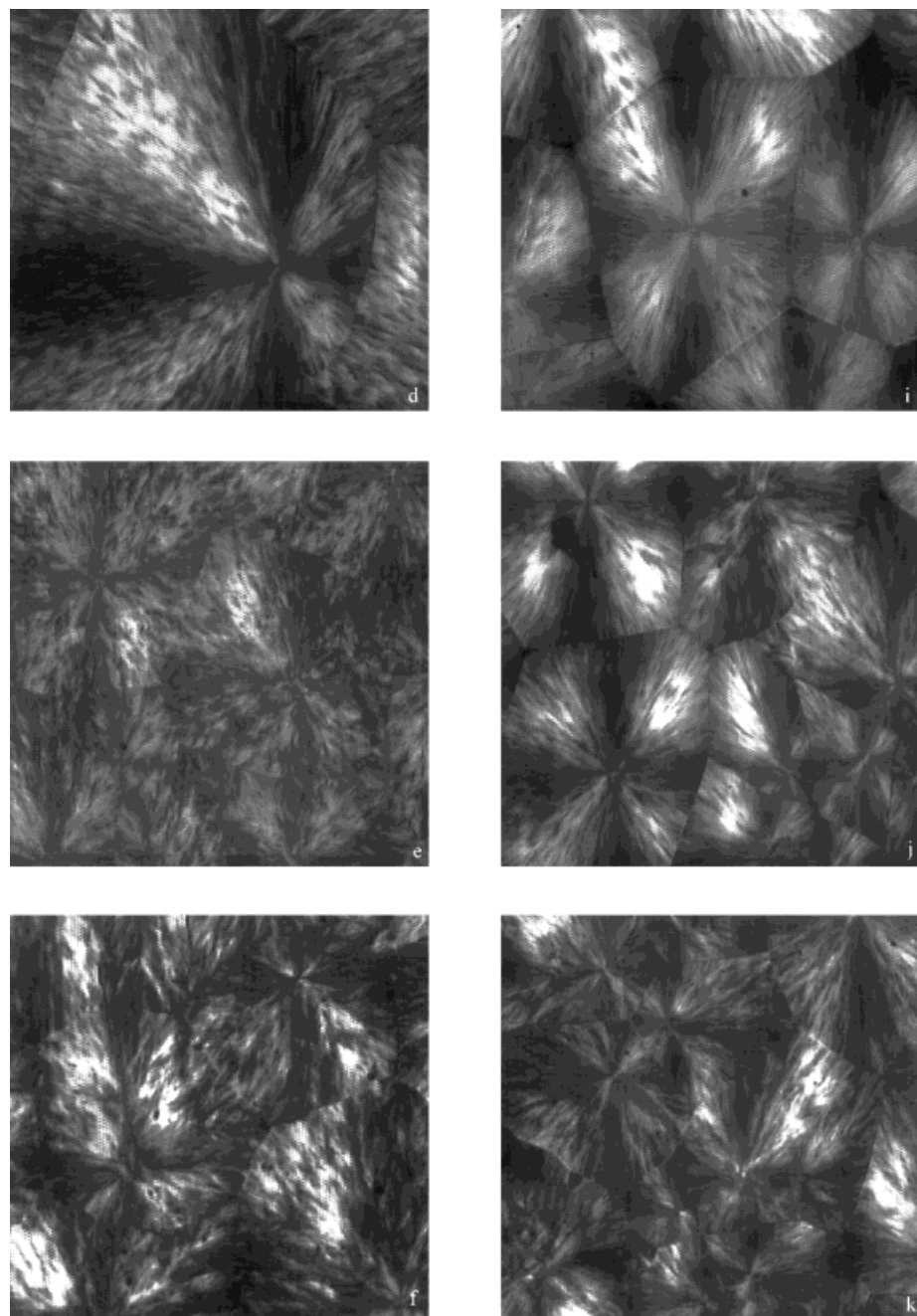


**Figure 4** (Continued from the previous page)

noted that the blends cast from chloroform showed greater values of  $t_{1/2}$  than those cast from benzene. This reconfirmed that PMMA showed a better ability to reduce the crystallization rate of PEO in the chloroform-cast blends.

From the DSC results, it showed that the casting solvent significantly influenced the crystallization of PEO. Thus the crystallization behavior and morphology of spherulite were studied by

POM. The optical micrographs of chloroform-cast blend films are shown in Figure 4(a–f). Those samples were isothermally crystallized at 44°C. The scales of optical micrographs were all the same. The results were similar to those reported by Martuscelli et al.<sup>28</sup> The blends used in ref. 28 were also cast from chloroform. Down to 50% PEO content, the blend films seem to be completely filled with PEO spherulites, truncated by im-

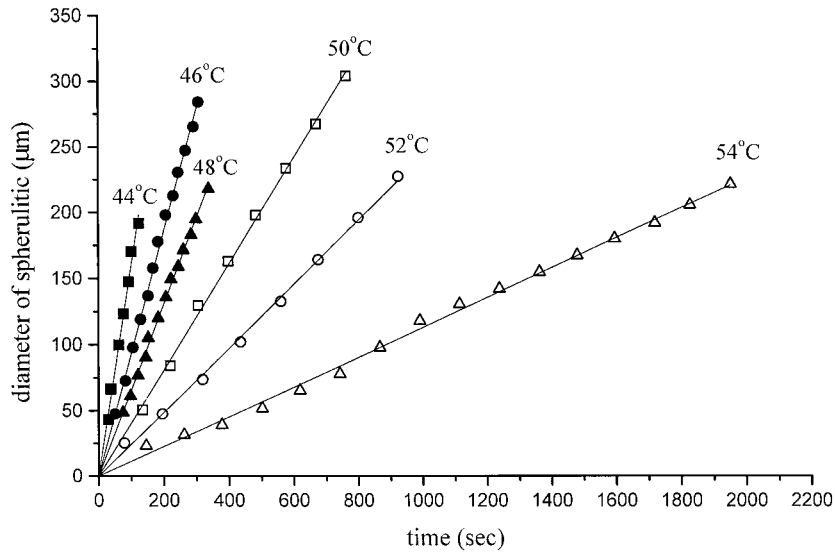


**Figure 5** Diameter of spherulite in benzene-cast PEO/PMMA (80/20) blend as a function of time for various crystallization temperatures.

pingement, and no separated domains of the amorphous phase were observed. It indicated that the noncrystallizable mixture was trapped into the interlamellar regions during the crystallization process. The conventional Maltese cross pattern was observed in these blend films. However, the cross pattern became more coarse and open with increasing the PMMA content. More inter-

esting was the effect of PMMA on the apparent nucleation density. Down to 80% PEO content, the apparent nucleation density of blend films was less than observed in the neat PEO film. The sizes of spherulites of blend films were larger than observed in the neat PEO blend film. Then, the apparent nucleation density increased with further addition of PMMA. On the other hand, the

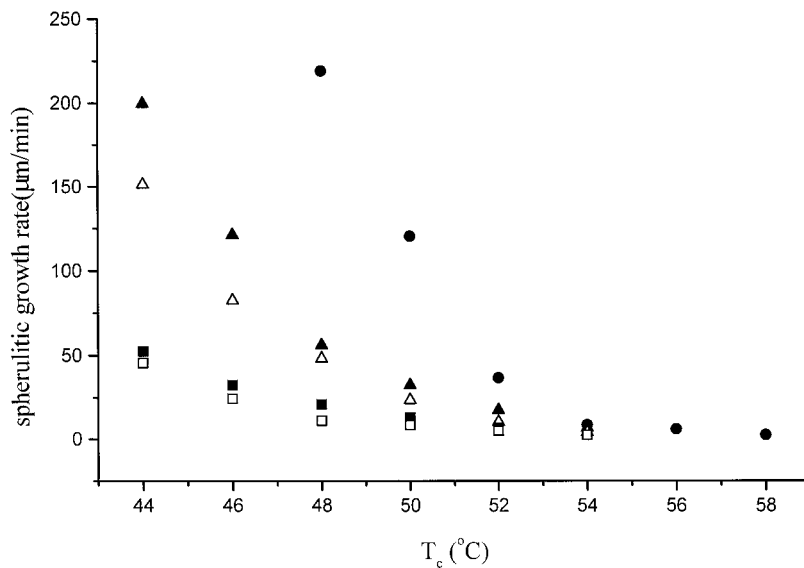


**Figure 6** Radial growth rate of spherulites in pure PEO and PEO/PMMA blends as a function of crystallization temperature. (●) pure PEO; (▲) 90/10 PEO/PMMA benzene-cast film; (△) 90/10 PEO/PMMA chloroform-cast film; (■) 80/20 PEO/PMMA benzene-cast film; (□) 80/20 PEO/PMMA chloroform-cast film.



size of spherulites decreased with increasing the PMMA content. The main way of primary nucleation present in this study was heterogeneous nucleation.<sup>31</sup> Bartzak and Martuscelli<sup>31</sup> suggested that the primary nucleation was depressed by the PMMA. However, PMMA only induced the inhibition of the less active nuclei. The more active nuclei in the blends remained active. Thus, the primary nucleation of blends with > 20% of PMMA was not further significantly depressed. On the other hand, PMMA could act as an impurity and induced heterogeneous nucleation of PEO crystallization. Thus, the nucleation density of blend films increased with increasing PMMA content. The combination of both factors caused the variation of apparent nucleation density in the blends with the variation of PMMA content. The optical micrographs of benzene-cast blend films are shown in Figure 4(g–k). Comparing the optical micrographs of benzene-cast and chloroform-cast films, it was found that the Maltese cross pattern of chloroform-cast film was coarser. It indicated that the chloroform-cast blends had more homogeneous morphology on microscopic scale in agreement with the DSC results. Down to 80% PEO content, the primary nucleation of benzene-cast blend was not significantly depressed as it was in the chloroform-cast blend. The inhibition of the primary nucleation in the benzene-cast blend might not be so efficient because of the less

homogeneous morphology than it was in the chloroform-cast blend. The results were in agreement with the DSC results.

Figure 5 is a typical plot of the diameter of PEO spherulite as a function of time for several isothermal crystallization temperatures in the 80/20 benzene-cast blend. It appeared that the slopes of these lines decreased with increasing the crystallization temperature. Furthermore, the growth rates of spherulites remained constant during the crystallization processes. It indicated that the concentration of PEO in the crystal growth front was constant during the crystallization, and the noncrystallizable materials were rejected and trapped into the interlamellae or interfibrils of spherulites. The results were in agreement with the observation of morphology. The spherulitic growth rates (i.e., slopes of lines) with crystallization temperature for PEO and its blends cast from benzene or chloroform solvent were shown in Figure 6. It was concluded that the spherulitic growth rates of chloroform-cast blends were less than those were in benzene-cast blends. Again, it indicated that the suppression of PEO crystallization in the benzene-cast blend was not so efficient as it was in the chloroform-cast blend due to the less homogeneous benzene-cast blend.

From the above discussion, it was shown that the casting solvent did influence the crystallization behavior and morphology of PEO. It was supposed

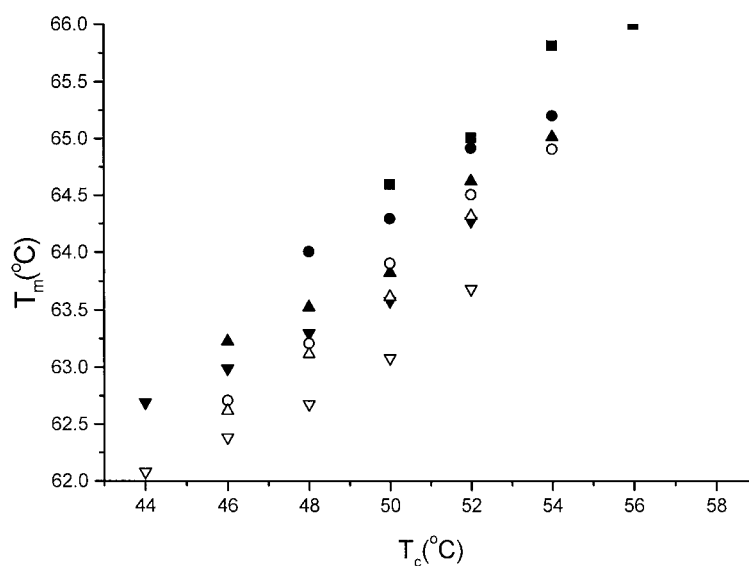


**Figure 7** The melting point versus crystallization temperature for PEO/PMMA blends. Solid symbols represent benzene-cast blends and open symbols represent chloroform-cast blends. (■) pure PEO; (●, ○) 90/10 PEO/PMMA; (▲, △) 80/20 PEO/PMMA; (▼, ▽) 70/30 PEO/PMMA.

that the chloroform-cast blend had more homogeneous morphology. Thus, the melting-point depressing of PEO crystal would be observed by POM. The melting point was the temperature at which the last spherulite disappeared. Figure 7 is the plot of melting temperature as a function temperature of crystallization temperature. As most of miscible blends, the melting-point depressing increased with increasing PMMA content. For the same composition and at the same crystallization temperature, the chloroform-cast blends had much larger melting depressing than observed in the benzene-cast blends. The results reconfirmed that chloroform-cast blends had more homogeneous morphology.

## CONCLUSION

From the depressing of crystallization rate and melting point and the single-composition-dependent  $T_g$  in the PEO/PMMA blends, it was concluded that PEO and PMMA were miscible in the molten state no matter which casting solvent was used in the whole composition range. However, from the suppression of crystallization, the half-time of crystallization, the morphology of spherulite, and the melting depressing, the chloroform-cast blends had more homogeneous morphology. It is fair to say that the polymer blends, cast from solvent, were not necessary in equilibrium. In this study, it was found that the benzene-cast blends still did not reach equilibrium even after preheating at 100°C for 10 min, which might be due to the high viscosity of the polymer blend at 100°C.

The authors acknowledge with gratitude financial support from the National Science Council, Taiwan, R.O.C., through Grant No. NSC86-2216-E-002-007.

## REFERENCES

- Paul, D. R.; Newman, S. *Polymer Blends*; Academic Press: New York, 1978.
- Olabisi, O.; Robeson, L. M.; Shaw, M. T. *Polymer-Polymer Miscibility*; Academic Press: New York, 1979.
- Calahorra, E.; Cortazar, M.; Guzman, G. M. *Polymer* 1982, 23, 1322.
- Alfonso, G. C.; Russell, T. P. *Macromolecules* 1986, 19, 1143.
- Russell, T. P.; Ito, H.; Wignall, G. D. *Macromolecules* 1988, 21, 1703.
- Li, X.; Hsu, S. L. *J Polym Sci, Polym Phys Ed* 1984, 22, 1331.
- Martuscelli, E.; Pracella, M.; Yue, W. P. *Polymer* 1984, 25, 1097.
- Silvestre, C.; Cimmino, S.; Martuscelli, E.; Karasz, F. E.; MacKnight, W. J. *Polymer* 1987, 28, 1190.
- Cimmino, S.; Pace, E. D.; Martuscelli, E.; Silvestre, C. *Makromol Chem Rapid Commun* 1988, 9, 261.
- Marcos, J. I.; Orlandi, E.; Zerbi, G. *Polymer* 1990, 31, 1899.
- John, E.; Ree, T. *J Polym Sci, Part A: Polym Chem* 1990, 28, 385.
- Wu, W. B.; Chiu, W. Y.; Liau, W. B. *J Appl Polym Sci* 1997, 64, 411.
- Radhakrishnan, S.; Venkatachalapathy, P. D. *Polymer* 1996, 37, 3749.
- Bank, M.; Leffingwell, J.; Thies, C. *Macromolecules* 1971, 4, 43.
- Cimmino, S.; Pace, E. D.; Martuscelli, E.; Silvestre, C. *Makromol Chem* 1990, 191, 22447.
- Tsitsilianis, C.; Staikos, G.; Dondos, A. *Polymer* 1992, 33, 3369.
- Friese, K. *Plast Kaut* 1968, 15, 646.
- Song, M.; Long, F. *Eur Polym J* 1991, 27, 983.
- Crispim, E. G.; Rubira, A. F.; Muniz, E. C. *Polymer* 1999, 40, 5129.
- Cheng, S. Z. D.; Wunderlich, B. *J Polym Sci, Polym Phys Ed* 1986, 24, 577.
- Kalfoglou, N. K. *J Polym Sci, Polym Phys Ed* 1982, 20, 1259.
- Kalfoglou, N. K.; Sotiropoulou, D. D.; Margaritis, A. G. *Eur Polym J* 1988, 4, 389.
- Martuscelli, E.; Silvestre, C.; Gismondi, C. *Makromol Chem* 1985, 186, 2161.
- Han, C. D.; Chung, H. S.; Kim, J. K. *Polymer* 1992, 33, 546.
- Cimmino, S.; Martuscelli, E.; Silvestre, C.; Canetti, M.; Lalla, C. D.; Seves, A. *J Polym Sci, Polym Phys Ed* 1989, 27, 1781.
- Guo, Q.; Peng, X.; Wang, Z. *Polymer* 1991, 32, 53.
- Nakafuku, C.; Sakoda, M. *Polym J* 1993, 25, 909.
- Martuscelli, E.; Silvestre, C.; Addonizio, M. L.; Amelino, L. *Makromol Chem* 1986, 187, 1557.
- Hoffman, D. M. Ph.D. Thesis, University of Massachusetts, Amherst, MA, 1979.
- Martuscelli, E.; Demma, G.; Rossi, E.; Segre, A. L. *Polym Commun* 1983, 24, 266.
- Bartczak, Z.; Martuscelli, E. *Makromol Chem* 1987, 188, 445.